

# Synergistic effects of polyhedral oligomeric silsesquioxane (POSS) and oligomeric bisphenyl A bis(diphenyl phosphate) (BDP) on thermal and flame retardant properties of polycarbonate

Qingliang He · Lei Song · Yuan Hu ·  
Shun Zhou

Received: 21 August 2008 / Accepted: 13 January 2009 / Published online: 7 February 2009  
© Springer Science+Business Media, LLC 2009

**Abstract** A series of flame retardant hybrids were prepared based on bisphenol A polycarbonate (PC), trisilanophenyl-polyhedral oligomeric silsesquioxane (TPOSS) and oligomeric bisphenyl A bis(diphenyl phosphate) (BDP) by melt blending method. The thermal stability and flame retardant properties of the hybrids were investigated by thermogravimetry analysis and cone calorimeter. Combination TPOSS with BDP in the appropriate ratio enhanced the thermal stability and the flame retardant properties of the PC matrix. The char residues of the hybrids were investigated by scan electronic microscopy (SEM) and X-ray photoelectron spectroscopy (XPS). The synergistic effect of BDP and TPOSS enhances the thermal stability and fire-resistance of the char layer which builds up on the surface of the burning polymer.

## Introduction

Bisphenol A polycarbonate (PC), one of the fastest growing engineering polymers, has excellent mechanical properties and excellent electrical properties, high glass transition temperature, heat distortion temperature and a wide temperature range, widely used in electrical and electronics, construction, packaging, medical equipment, optical equipment, aerospace, computers, transport, and other fields [1].

In the recent years, the thermal degradation behavior and mechanism of PC had been investigated in detail [2–10]. More than 40 years ago, Lee [2] had studied the thermal decomposition of bisphenol A polycarbonate, and postulated a radical cleavage of the polymer chain at the carbonate bonds that described well the commonly observed formation of bisphenol A, phenyl isopropyl phenol, and carbon dioxide from PC [3]. Later several decompositions and side reactions have been reported, namely, oligomeric ring formation under vacuum [4], elimination leading to ethers, and isomerization producing xanthone structures [3, 5–7].

For the flame retardant properties of PC, it shows a V-2 rating in the UL-94 test because PC is a naturally high charring polymer, but strict flame retardant performance is often required for electronic and electric applications, the flame retardant technologies of polycarbonate have been developed [8–10]. Many academic and industrial researchers have participated in the study of flame retardancy of PC and its blends [8]. The effective halogen-free flame retardants for PC include some phosphorus-, sulfur-, and silicone-based flame retardants [8]. BDP is one of the important phosphorus flame retardants, with high thermal stability, oxidation resistance, and excellent water resistance. Because of its high compatibility with the polymer matrix, resistance movements, volatile resistant and good thermal stability, it was widely used in many high-performance polymers. Pawlowski and Schartel [11] investigated the thermal decomposition and the pyrolysis behavior of aryl phosphates (TPP, RDP, and BDP) in PC/ABS. It was found the combination of gas and condensed phase action of BDP results in a slightly superior performance in terms of fire load and decreasing the flame spread [11].

Fina et al. [12] investigated the thermal degradation of several substituted polyhedral oligomeric silsesquioxanes

Q. He · L. Song (✉) · Y. Hu (✉) · S. Zhou  
State Key Laboratory of Fire Science, University of Science  
and Technology of China, Hefei 230026,  
Anhui, People's Republic of China  
e-mail: leisong@ustc.edu.cn

Y. Hu  
e-mail: yuanhu@ustc.edu.cn

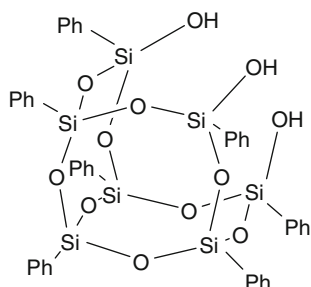
(POSS). Phenyl-substituted POSS shows a higher thermal stability than saturated aliphatic POSS and limited volatility, producing a ceramic residue at high yield on heating. The incorporation of POSS which is regarded as a nano-scale filler is expected to lead to new or enhanced properties [13–15]. The preparations, morphology, crystallization, rheological behaviors, mechanical, thermal and flame retardant properties of the hybrids were reported. Zhao and Schiraldi [15] studied the mechanical properties of PC/POSS derivatives/composites. They found the mechanical properties including tensile and dynamic mechanical modulus were slightly enhanced with the increase of trisilanophenyl-POSS loading. Trisilanophenyl-POSS were shown to be more compatible with PC than fillers with other functional groups.

In our previous article, POSS was found to significantly affect the thermal degradation and combustion behaviors of PC [16]. In this article, the synergistic effects of POSS and BDP on the thermal stability and flame retardant properties of polycarbonate were investigated.

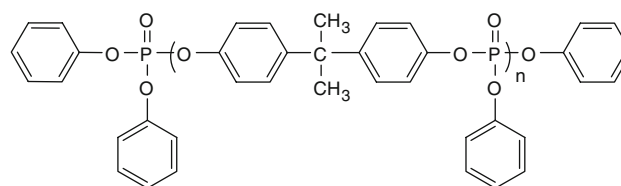
## Experimental part

### Materials

Bisphenol A polycarbonate (PC) used in our study was obtained as pellets from Dow Chemical Company. The polyhedral oligomeric silsesquioxane (POSS) we used was SO1458, TriSilanolPhenyl-POSS ( $C_{42}H_{38}O_{12}Si_7$ , molecular weight = 931.34 g/mol), chemical name is 1,3,5,7,9,11,14-Heptaphenyltricyclo[7.3.3.1(5,110)] heptasiloxane-endo-3,7,14-triol, and was purchased from Hybrid Plastics Inc. Scheme 1 shows the structures of the TriSilanolPhenyl-POSS (TPOSS) molecule; TPOSS contains a partial T8 cage with one corner Si missing, leaving three Si–OH groups. Oligomeric bisphenyl A bis(diphenyl phosphate) (BDP) was received from Yoke Chemical Co. Ltd., China. Scheme 2 shows the structures of BDP. The polymer was dried for 24 h in a circulating air oven at 100 °C prior to use, whereas TPOSS and BDP were used as received.



**Scheme 1** The structure of TPOSS



**Scheme 2** The structure of BDP

### Preparation of samples

PC pellets and various contents of BDP were melt-mixed at 280 °C in a twin-roll mill (XK-160, made in Jiangsu, China). Then TPOSS was added to the mixture, and blended for 10 min with the rotational speed of 30 rpm. Finally, the PC/BDP/TPOSS hybrids were obtained. The slab-shaped specimens for the CONE tests were prepared by compressing at 290 °C under a pressure of 10 MPa in a 10 cm × 10 cm × 3 mm mold for 5 min. The pure PC used as a standard was treated in the same way. The compositions of the formulations are shown in Table 1.

### Characterization

The compatibility of TPOSS in hybrids was evaluated by means of transmission electron microscopy (TEM). The samples were cut from epoxy blocks with the embedded samples at room temperature using an ultramicrotome (Ultracut-1, UK) with a diamond knife. Thin sections, 50–80 nm, were collected with 200-mesh copper grids in a trough filled with water. TEM images were obtained with a Hitachi H-800 microscope at an acceleration voltage of 100 kV. TPOSS molecule has a Si–O core covered with seven phenyl groups and three hydroxyl groups; it is believed that better dispersion may result from the chemical bonding of hydroxyl groups and increased interaction of compatible side groups with PC.

Thermogravimetric analysis (TGA) and differential thermal analysis (DTA) were carried out using a Netzsch STA-409C thermal analyzer. Samples weighting about

**Table 1** The compositions of the formulations

Samples	PC (wt%)	BDP (wt%)	TPOSS (wt%)
PC0	100	0	0
PC1	97	3	0
PC2	95	5	0
PC3	96	3	1
PC4	95	3	2
PC5	94	3	3

10 mg, and measurements were performed from room temperature to 800 °C at a heating rate of 10 °C/min.

The cone calorimeter experiments were performed according to the procedure defined in ISO 5660, on the 3 mm thick 100 × 100 mm<sup>2</sup> plaques, using the cone-shaped heater. Heat release rate and mass loss rate were obtained from the cone calorimetry experiment using an on-line software. Typical results from cone calorimeter were reproducible within ± 10% at a heat flux of 50 kW/m<sup>2</sup>.

The morphology of char was observed by scanning electron microscopy (SEM) using the JSM-6700F apparatus. The specimens were previously coated with a conductive layer of gold. And the char was characterized by X-ray photoelectron spectroscopy (XPS) which was carried out with a VG Escalab mark II spectrometer (VG Scientific Ltd, UK), using Al K $\alpha$  excitation radiation ( $h\nu = 1253.6$  eV).

## Results and discussion

### Morphology of PC/BDP/TPOSS hybrids

Figure 1 shows TEM image of PC/2 wt%TPOSS/3 wt%BDP hybrid with the contents of 2 wt%TPOSS and 3 wt% BDP. BDP is a liquid at room temperature and its invisibility is investigated by TEM. The image can provide the information about the size-scale level, the dispersion, and morphology of TPOSS in the PC matrix. Figure 1 shows TPOSS in the shape of an elongated ellipsoidal particle with a length of 200 nm to 1  $\mu$ m and a width of 20–200 nm dispersed in the PC matrix as TPOSS and BDP both incorporated in PC. This maybe results from the incorporation of the liquid BDP. TPOSS is more compatible with BDP than with the PC matrix. The solid particles

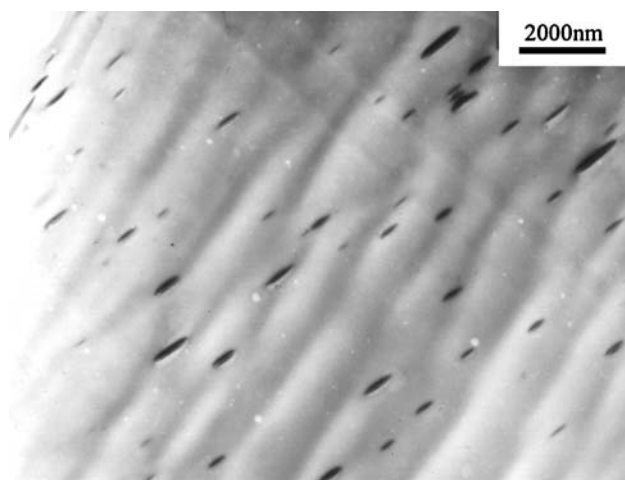


**Fig. 1** TEM image of the dispersion of TPOSS in PC/3 wt%BDP/2 wt%TPOSS hybrid

of TPOSS dissolve in the liquid BDP during preparation process. The liquid-drop of BDP was elongated by the shear force of melt blending equipment during the preparation process. Then TPOSS re-crystallizes from the liquid BDP with temperature of hybrid decreasing after the preparation. So the morphology of TPOSS shows the shape of distorted ellipsoidal particle.

### Thermal properties of hybrids

#### Thermogravimetric analysis in inert atmosphere

The TGA curves and the detailed data of pure PC, PC3 wt%BDP, PC/5 wt%BDP, PC/3 wt%BDP/1 wt%TPOSS, PC/3 wt%BDP/2 wt%TPOSS, and PC/3 wt%BDP/3 wt%TPOSS in N<sub>2</sub> atmosphere are shown in Fig. 2a, b and Table 2, respectively. The onset degradation temperature of samples was evaluated by the temperature of 5 wt% weight loss ( $T_{-5\%}$ ), the mid-point temperature of the degradation ( $T_{-50\%}$ ), the temperature of 70 wt% weight loss ( $T_{-70\%}$ ), the

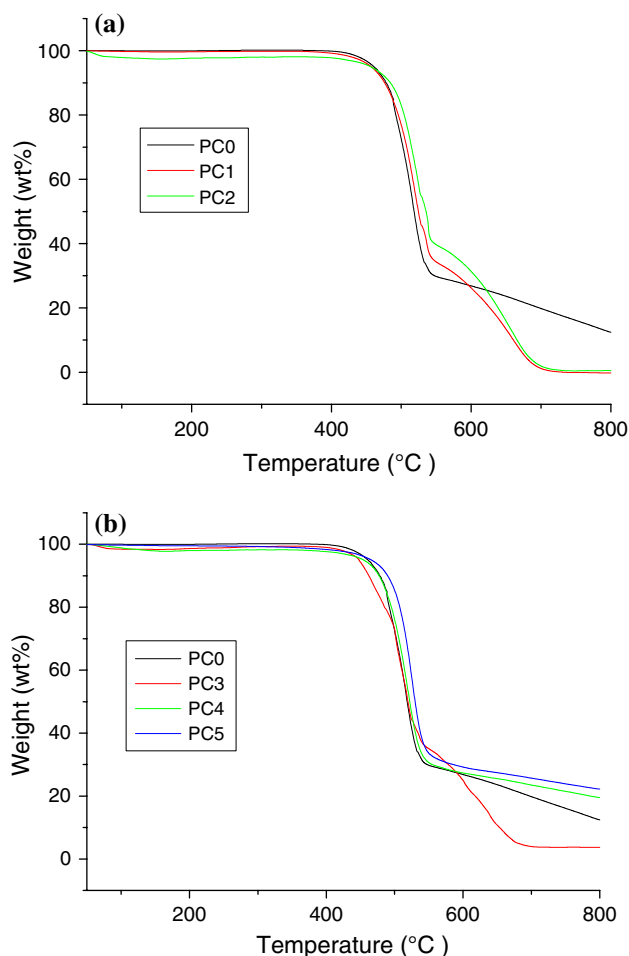


**Fig. 2** TGA curves of **a** PC and PC/BDP series hybrids and **b** PC/BDP/TPOSS series hybrids under inert atmosphere

**Table 2** TG, DTG data of the hybrids (N<sub>2</sub>)

Samples	$T_{-5\%}$ (°C)	$T_{-50\%}$ (°C)	$T_{-70\%}$ (°C)	$T_{-90\%}$ (°C)	Char (%)	$T_{\max}$ (°C)
PC0	461.0	518.3	502.5	>800	12.43	516.3
PC1	457.1	524.4	507.8	660.4	0	518.5 653.5
PC2	456.5	535.4	514.7	665.8	0.540	523.1 654.8
PC3	447.9	519.4	501.6	653.6	3.69	511.8 634.7
PC4	454.5	522.1	506.3	>800	19.51	519.1
PC5	466.0	529.9	516.8	>800	22.2	525.4

temperature of 90 wt% weight loss ( $T_{-90\%}$ ), and the fraction of the char residue (CHAR) that does not volatilize below 800 °C were obtained from the TG curve. The differential analysis of the TGA curves of all the samples gives the temperatures of the maximum weight loss rate ( $T_{\max}$ ) which are all listed in Table 2.

The thermal degradation process of pure PC exhibits one step in the inert atmosphere. The major degradation of pure PC occurred between 460 and 550 °C:  $T_{-5\%}$  is 461 °C, and the  $T_{\max}$  is 523.6 °C. Some complex chemical reactions take place during the thermal degradation of PC, which include the chain scission of the isopropylidene linkage, hydrolysis/alcoholysis of carbonate linkage, reformation of carbonate linkage, and branching and crosslinking reaction of the molecular chains of PC [6]. Then the crosslinking polyaromatic carbonaceous residue is formed via crosslinking reactions at the higher temperature. The char residue of pure PC at 800 °C in the N<sub>2</sub> atmosphere was 12.43 wt%.

The degradation process of PC/BDP series hybrids becomes two-step because of the presence of BDP.  $T_{-5\%}$  of the PC/BDP series hybrids is lower than that of PC and tends to decrease with the increase of BDP content. Although  $T_{-50\%}$ ,  $T_{-70\%}$ , and  $T_{\max}$  are all higher than that of PC,  $T_{-90\%}$  of PC/BDP series hybrids is much lower than that of the pure PC, and there is no content left at 800 °C in the N<sub>2</sub> atmosphere. Incorporation of BDP decreases the thermal stability of the PC matrix.

The thermal degradation process of PC3 also has two steps similar to that of PC1.  $T_{-5\%}$ ,  $T_{-50\%}$ ,  $T_{-70\%}$ ,  $T_{-90\%}$ , and  $T_{\max}$  of PC3 Combining 1 wt% TPOSS with 3 wt% BDP are lower than that of PC1; Only CHAR is slight higher than that of PC1. And those data are all lower than that of the pure PC except for  $T_{-50\%}$ . The thermal degradation process of the other PC/BDP/TPOSS series hybrids becomes one step with the TPOSS content increasing which is different from the PC/BDP series hybrids. TPOSS  $T_{-5\%}$ ,  $T_{-50\%}$ ,  $T_{-70\%}$ , and  $T_{\max}$  of PC4 are lower than that

of PC/BDP series hybrid; and  $T_{-90\%}$  and CHAR are higher than that of PC/BDP series hybrid. Moreover, those data of PC4 are all higher than that of pure PC except for  $T_{-5\%}$ .  $T_{-5\%}$ ,  $T_{-50\%}$ ,  $T_{-70\%}$ ,  $T_{-90\%}$ , CHAR, and  $T_{\max}$  of PC/BDP/TPOSS series hybrids all increase with the TPOSS content increasing. Those data of PC5 are all higher than that of pure PC and PC/BDP series hybrid except for  $T_{-50\%}$ . Combination TPOSS with BDP decreases the thermal degradation stability of hybrids at lower temperature and increase the thermal degradation stability at higher temperature in the inert atmosphere compared with that of PC/BDP series hybrids. However, combination TPOSS with BDP in appropriate ratio can increase the thermal degradation stability not only at higher temperature but also lower temperature compared with pure PC and PC/BDP series hybrids. The enhancement of thermal stability is probably due to the synergistic effect between TPOSS and BDP.

#### Thermogravimetric analysis in air

TGA curves and the detailed data of pure PC, PC3 wt%BDP, PC/5 wt%BDP, PC/3 wt%BDP/1 wt%TPOSS, PC/3 wt%BDP/2 wt%TPOSS, PC/3 wt%BDP/3 wt%TPOSS in air are shown in Fig. 3a, b and Table 3, respectively. The onset degradation temperature of samples was evaluated by the temperature of 5 wt% weight loss ( $T_{-5\%}$ ), the mid-point temperature of the degradation ( $T_{-50\%}$ ), the temperature of 70 wt% weight loss ( $T_{-70\%}$ ), the temperature of 90 wt% weight loss ( $T_{-90\%}$ ), and the fraction of the char residue (CHAR) that does not volatilize below 800 °C were obtained from the TG curve. The TGA curves of all the samples exhibit that their thermo-oxidative degradation processes had two steps. The differential analysis of the TGA curves of all the samples give two temperatures of the maximum weight loss rate ( $T_{\max1}$  and  $T_{\max2}$ ) corresponding to two steps of the thermo-oxidative degradation processes. These data are all listed in Table 3.

The onset degradation temperature of the pure PC, namely PC0 is 430.4 °C. The first step of the thermo-oxidative degradation is in the temperature range of 50–550 °C and  $T_{\max1}$  is at 501.2 °C. The second step of degradation is between 550 and 800 °C;  $T_{\max2}$  is at 616.8 °C. Pure PC has not left any char residue at 800 °C. From the TGA results in both air and inert atmosphere, it can be speculated that the presence of oxygen accelerates the degradation of PC matrix.

For the hybrids with only BDP, namely, PC1 and PC2, the two steps are in the temperature ranges of about 50–550 and 550–800 °C, respectively. For PC1,  $T_{\max1}$  increases by 13.6 °C, but  $T_{\max2}$  decreases by 4.5 °C compared with pure PC; the addition of 3 wt% BDP results in  $T_{-5\%}$ ,  $T_{-50\%}$ ,

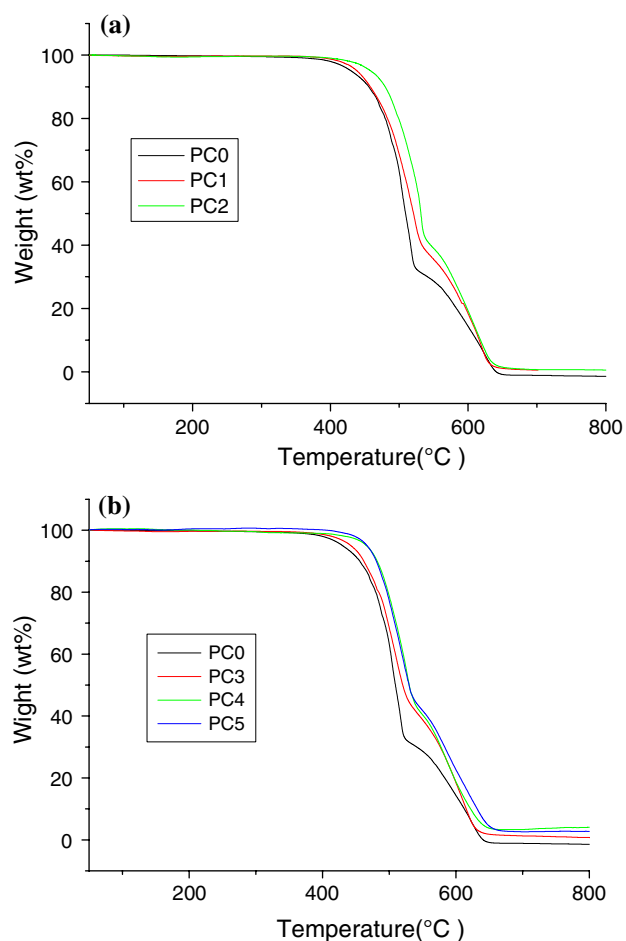


**Fig. 3** TGA curves of **a** PC and PC/BDP series hybrids and **b** PC/TPOSS series hybrids under air atmosphere

**Table 3** TG, DTG data of the hybrids (air)

Samples	$T_{-5\%}$ (°C)	$T_{-50\%}$ (°C)	$T_{-70\%}$ (°C)	$T_{-90\%}$ (°C)	CHAR (%)	$T_{\max}$ (°C)
PC0	430.4	509.2	541.1	612.3	0	501.2 616.8
PC1	438.8	520.6	569.9	616.2	0	514.8 612.3
PC2	458.7	531.4	577.2	617.9	0	524.5 610.7
PC3	442.7	520.2	576.4	615.3	0.75	502.9 602.8
PC4	466.0	530.0	577.5	621.9	4.07	520.8 583.9
PC5	466.9	529.7	583.0	631.8	2.77	517.2 596.1

$T_{-70\%}$ , and  $T_{-90\%}$  increase 8.4, 11.4, 28.8, and 3.9 °C, respectively. With the amount of BDP increasing from 3 to 5 wt% for PC2,  $T_{-5\%}$ ,  $T_{-50\%}$ ,  $T_{-70\%}$ , and  $T_{-90\%}$  all

increase 19.9, 10.8, 7.3, and 1.7 °C, respectively;  $T_{\max1}$  increases by 9.7 °C and  $T_{\max2}$  decreases compared with PC1. However, addition of BDP cannot result in the formation of the stable char residue at 800 °C. These indicate that the incorporation of BDP in PC can enhance the thermo-stability of PC in the first degradation step with the temperature increasing; and this enhancement effect has been weakened with the temperature increasing in the second degradation step.

Incorporation of 1 wt% TPOSS and 3 wt% BDP for PC3 results in  $T_{-5\%}$  and  $T_{-70\%}$  slight increase of 3.9 and 6.5 °C,  $T_{-50\%}$ , and  $T_{-90\%}$  slight decrease, and  $T_{\max1}$  and  $T_{\max2}$  obvious decrease compared with that of PC1; with the amount of TPOSS increasing from 1 to 2 wt% for PC4,  $T_{-5\%}$ ,  $T_{-50\%}$ ,  $T_{-70\%}$ ,  $T_{-90\%}$ , and  $T_{\max1}$  all obviously increase,  $T_{\max2}$  further decreases compared with PC1 and PC3. With the amount of TPOSS increasing from 2 to 3 wt% for PC5,  $T_{-10\%}$ ,  $T_{-50\%}$ , and  $T_{\max1}$  show a slight decrease, and  $T_{-70\%}$ ,  $T_{-90\%}$ , and  $T_{\max2}$  show further increase compared with PC4. Moreover, the addition of TPOSS results in the formation of a few char residues at 800 °C. Comparing the thermo-oxidative stability of PC4 with that of PC2 with the same additive content,  $T_{-5\%}$  and  $T_{-90\%}$  of PC4 are higher than those of PC2;  $T_{\max1}$  and  $T_{\max2}$  are both lower than those of PC2. And the char residue of PC4 at 800 °C was 4.07 wt% while PC2 had not left any char residue at 800 °C.

From above data, it is clear that the introduction of BDP obviously enhances the thermo-oxidative stability of the PC matrix. And the combination TPOSS with BDP can further enhance the thermo-oxidative stability of the PC matrix, especially with regard to increase of the onset degradation temperature and amount of char formation.

#### Flame retardant properties of hybrids

The cone calorimeter was a useful tool for fire safety engineers and researchers interested in quantitative analysis of material flammability. It remains as one of the most useful bench-scale tests that attempts to simulate real fire conditions. The cone calorimeter enables quantitative analysis of materials flammability research through investigating parameters such as heat release rate (HRR), time to ignition ( $t_{\text{ign}}$ ), total heat release (THR), and mass loss rate (MLR) [17]. The heat release rate (HRR) was measured by cone calorimeter; HRR peak (PHRR) has been considered to be the most important parameter to evaluate the fire safety characteristics of polymeric materials. Methane in the volatile products of PC is a highly volatile as well as a highly combustible gas, which is the major fuel supporting the ignition and combustion of PC [8]. Figure 4a shows that the combustion process of pure PC presents a sharp peak on the HRR curve, but the value of PHRR is only

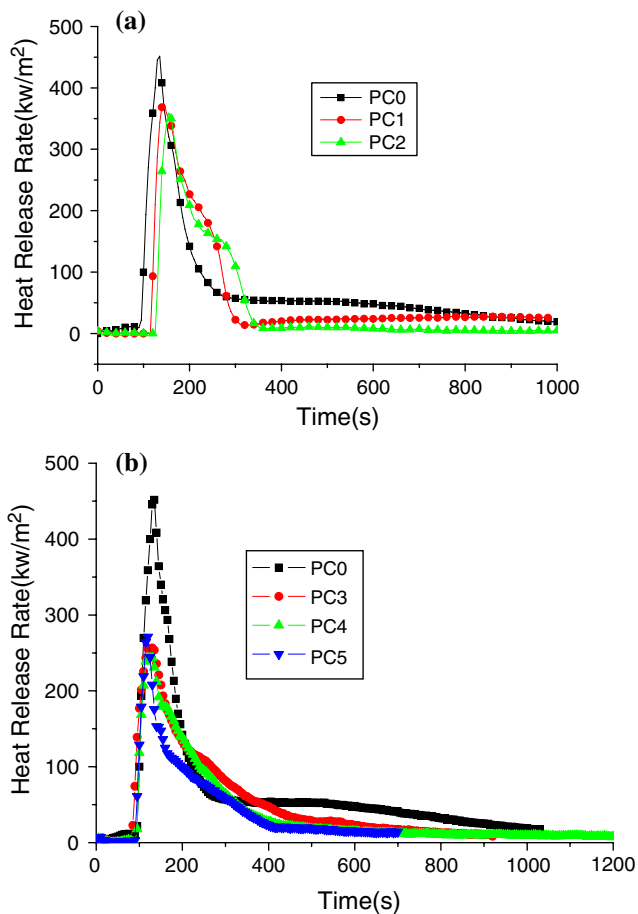


**Fig. 4** HRR plots of **a** PC and PC/BDP series hybrids and **b** PC/BDP/TPOSS series hybrids

451.7 kW/m<sup>2</sup> under a heat flux of 50 kW/m<sup>2</sup>. The pure PC is charred rapidly and decomposed slowly under the heat; after ignition, the sample is burnt slowly and charred rapidly during the combustion; many char residues are formed on the surface of sample so that the flame becomes very small and this kind of combustion with small flame can sustain longer than 10 min. Figure 4a shows that the combustion process of the PC/BDP series hybrids presents

an obvious shoulder peak after the sharp peak at the combustion time of 200–400 s and the value of PHRR is lower than that of pure PC; moreover, the ignition of the PC/BDP series hybrids is retarded; and the phenomenon of combustion is similar to that of pure PC. Figure 4b shows that the combustion process of the PC/BDP/TPOSS series hybrids presents only a peak and the value of PHRR is further reduced compared with that of the PC/BDP series hybrids; however, the ignition of them is advanced; and the phenomenon of combustion is different from that of the pure PC. The sample is charred and decomposed rapidly under the heat so that the ignition of sample is advanced; After the ignition, the sample is burnt slowly and charred rapidly; many char residues are formed on the surface of the sample; many volatile products are released from the sample under the charred residue simultaneously so that the char residue is swelled to form a porous charred layer which probably results in the smaller value of HRR.

Table 4 lists some cone data of all the samples including the time of ignition ( $t_{ign}$ ), the values of the peak and average of HRR and MLR, and the values of the THR. The addition of BDP results in the values of  $t_{ign}$ , PHRR, AvHRR, and THR increasing for PC/BDP series hybrids compared with that of pure PC. And those values increase with the content of BDP increasing. However, the addition of BDP hardly affects the values of PMLR and AvMLR. Incorporation of TPOSS with BDP into the PC matrix for PC/BDP/TPOSS series hybrids results in the values of those values decreasing at an appropriate ratio of BDP and TPOSS compared with PC/BDP series hybrids which are favorable factors for the flame retardancy of PC. And the maximum reduction in PHRR, AvHRR, PMLR, and AvMLR is achieved at the ratio of 2 wt%TPOSS and 3 wt% BDP. Moreover, combination of BDP and TPOSS results in the values of  $t_{ign}$  decreasing which is unfavorable factor for the flame retardancy of PC. As concluded from Table 4 and Fig. 3a, b, the presence of both TPOSS and BDP at an optional ratio results in a great improvement in the flame retardancy. These might be due to the synergistic effect between BDP and TPOSS in the PC matrix.

**Table 4** Cone calorimetric data of the samples

Samples	PC	PC/ 3 wt%BDP	PC/ 5 wt%BDP	PC/3 wt%BDP/ 1 wt%TPOSS	PC/3 wt%BDP/ 2 wt%TPOSS	PC/3 wt%BDP/ 3 wt%TPOSS
$t_{ign}$ (s)	92	110	128	80	94	91
HRR (kW/m <sup>2</sup> )						
Peak	451.7	372.42	359.0	256.5	243.6	271.3
Average	75.54	62.58	42.14	58.92	31.74	54.73
MLR (g/m <sup>2</sup> s)						
Peak	0.244	0.229	0.238	0.159	0.157	0.181
Average	0.026	0.031	0.028	0.032	0.017	0.026
THR (MJ/m <sup>2</sup> )	66.4	53.8	42.9	49.7	46.0	33.5

## SEM analysis

The microstructures of char residues left by the samples after cone tests were investigated by Scanning electron microscopy (SEM) observation. Figure 5 gives the morphology of the exterior char residue of the pure PC,

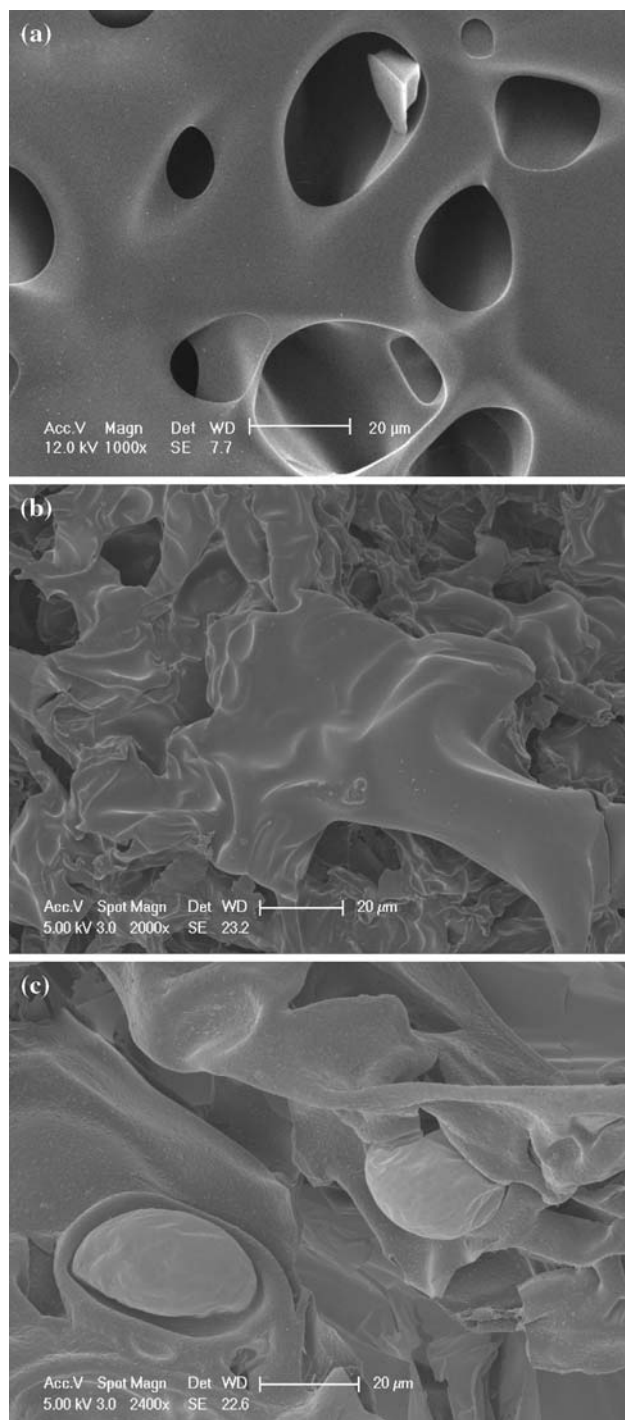


**Fig. 5** SEM images of the exterior char residues of **a** PC, **b** PC/3 wt%BDP, **c** PC/3 wt%BDP/2 wt%TPOSS

PC/3 wt%BDP hybrid, and PC/2 wt%TPOSS/3 wt%BDP. The exterior char residue of the pure PC presents a porous char layer with many micro-sized pores. This means that the rapid volatilization has happened in the PC matrix because of the heat. The exterior char residues of PC/3 wt%BDP and PC/2 wt%TPOSS/3 wt%BDP both present a rough char layer with some holes, cracks, and ridges formed by the inflatable and leakage bubbles. The addition of BDP or BDP and TPOSS restricts the rapid volatilization in the PC matrix and enhances the flame resistance of the exterior char residue.

## XPS spectra analysis

The XPS spectra analysis gives further information of the char residue on the chemical changes concerned [3]. The exterior and interior char residues of the pure PC, PC/3 wt%BDP, and PC/3 wt%BDP/2 wt%TPOSS are investigated by XPS analysis. The C 1s, O 1s, Si 2p, and P 2p spectra of samples are shown in Table 5. The C 1s spectrum of the pure PC has four peaks [18]: the peak at around 284.7 eV is attributed to C–H and C–C in aromatic species, the peak at around 286.3 eV assigned to C–O (ether and/or hydroxyl group), and the other two peaks corresponded to carbonyl (at around 287.7 eV) and carboxyl (at around 289 eV) groups. For O 1s spectrum, pure PC has two peaks, around 531.5 eV assigned to =O in carbonyl groups and 533.6 eV assigned to –O– in C–O groups.

For the pure PC, the atom percent of oxygen in the exterior char residue is higher than that in the interior char residue. And the atom percent of carbon in aromatic species in the exterior char residue is lower than that in the interior char residue. Those phenomena, probably due to the exterior char residue, are highly oxidized under the oxygen-rich condition. In addition, the pure PC has a weak peak on Si 2p at around 102.6 eV assigned to Si–O in the exterior char residue. The atom percent of Si is only 0.25% which probably is derived from the processing agent.

For the PC/3 wt%BDP hybrid, the atom percents of carbon, oxygen, and phosphorus in the exterior and interior char residues are all listed in Table 5. The atom percent of P in the exterior and interior char residues is 1.26% and 0.53%, respectively. Obviously, the content of P in the exterior char residue is much higher than that in the interior char residue. This result implies that P can be accumulated at the surface of burning PC matrix. It is known that the phosphorus-containing flame retardants (BDP) can react with the degradation products of PC, and then reside in the char layer on the polymer surface which can enhance the thermal-oxidative stability and retards the oxidation of the matrix. However, the ratios between unoxidized carbon and oxidized carbon of PC/3 wt%BDP hybrid are slightly lower than that of PC in the exterior char residues. This

**Table 5** XPS data of the samples

Exterior char residue			Interior char residue		
PC	Binding energy (eV)	Area (%)	PC	Binding energy (eV)	Area (%)
C 1s (C–H, C–C)	284.74	56.36	C 1s (C–H, C–C)	284.65	80.45
C 1s (C–O)	286.29	17.13	C 1s (C–O)	286.28	6.1
C 1s (C=O)	288.74	5.02	C 1s (C=O)	288.52	4.78
O 1s	533.11	17.23	O 1s	533.21	8.66
Si 2p	102.61	0.25	Si 2p	0	0
Exterior char residue			Interior char residue		
PC/3 wt%BDP	Binding energy (eV)	Area (%)	PC/3 wt%BDP	Binding energy (eV)	Area (%)
C 1s (C–H, C–C)	284.73	52.96	C 1s (C–H, C–C)	284.65	61.29
C 1s (C–O)	286.24	18.08	C 1s (C–O)	286.11	18.34
C 1s (C=O)	288.37	5.1	C 1s (C=O)	288.64	5.16
Si 2p	103	0.57	Si 2p	0	0
P 2p	133.87	1.26	P 2p	134.07	0.53
O 1s	533.26	22.03	O 1s	533.06	14.68
Exterior char residue			Interior char residue		
PC/2 wt%TPOSS/ 3 wt%BDP	Binding energy (eV)	Area (%)	PC/2 wt%TPOSS/ 3 wt%BDP	Binding energy (eV)	Area (%)
C 1s (C–H, C–C)	284.65	50.07	C 1s (C–H, C–C)	284.59	71.79
C 1s (C–O)	286.34	7.46	C 1s (C–O)	286.32	6.43
C 1s (C=O)	287.3	5.23	C 1s (C=O)	288.71	4.60
Si 2p	103.24	5.59	Si 2p	103.24	0.53
P 2p	134.23	1.57	P 2p	133.49	0.32
O 1s	532.89	30.09	O 1s	533.22	16.32

indicates that BDP cannot improve the thermal-oxidative stability of the char layer.

For the PC/2 wt%TPOSS/3 wt%BDP hybrid, the atom percents of both Si and P in exterior char residue are much higher than that in the interior char residue. This result implies that SiO<sub>2</sub> derived from TPOSS can be accumulated or pushed by the volatile product on the surface of burning PC. Moreover, the ratio of P content in exterior char residues is much higher than the ratio of pure PC and PC/3 wt%BDP hybrid. This is probably due to the reaction between P and Si on the surface of the burning PC matrix. SiO<sub>2</sub> reacts easily with phosphate to yield silico-phosphate, which is known to stabilize phosphorus species [19–24]. The ratios between unoxidized carbon and oxidized carbon of PC/3 wt%BDP/2 wt%TPOSS are higher than that of PC in exterior char residues. It indicates that the incorporation of TPOSS improves the thermal-oxidative stability and retards the oxidation of char layer on the surface of the matrix.

During the combustion process, the thermal-oxidative degradation of PC matrix proceeds very quickly and violently under a high temperature. This process is not similar

to that of TGA in air atmosphere. The synergistic effect of TPOSS and BDP on combustion behaviors could be summarized: Under the high temperature, a char layer is formed on the surface of the matrix; a fast degradation is preceded in the matrix. BDP decomposes and volatilizes to provide the gas flame retardant effect in the gas. BDP can participate in the formation of char layer on the surface of the matrix. At the same time, TPOSS quickly undergoes a series of oxidation reactions to form SiO<sub>2</sub> in the matrix and releases more combustible small molecules such as benzene dissociated from TPOSS. So the time for ignition of hybrids decreases. Quite a few SiO<sub>2</sub> molecules are pushed to the surface of the matrix by the volatile products such as phenol derivatives, methane, CO, and CO<sub>2</sub>. And SiO<sub>2</sub> reacts with phosphate residing in char layer to yield silico-phosphate, which can stabilize phosphorus species and char layer. The presence of SiO<sub>2</sub> can further enhance the viscosity and thermal-oxidative stability of the char layer containing phosphorous which builds up on the surface of the burning polymer, insulates the heat transformation, and caused the dispersion of oxygen into underlying polymeric substrate to prevent thermo-oxidative reactions, and also

prevents the release of volatile products of underlying polymeric substrate from the matrix. So the value of HRR of hybrids decreases. The competitive effects of TPOSS on the improvement of the amount of combustible small molecules at the early stage of the combustion and enhancement of viscosity and stability of the char layer result in a balance for synergistic flame retardant effect of TPOSS and BDP.

## Conclusion

PC/TPOSS/BDP hybrids were prepared based on bisphenol A polycarbonate (PC), trisilanolphenyl-POSS (TPOSS), and oligomeric bisphenyl A bis(diphenyl phosphate) (BDP) by melt blending. The thermal stability and the flame retardant properties of the PC/TPOSS/BDP hybrids were investigated. The addition of TPOSS and BDP significantly affect the thermal degradation and combustion behaviors. The results indicated that combination TPOSS with BDP in the optimal ratio can enhance the thermal stability of the PC matrix under inert and air atmosphere. The addition of both TPOSS and BDP significantly improves the flame retardant properties of the hybrids, more than the addition of BDP alone. The synergistic effect of BDP and TPOSS significantly decreased the value of peak heat release rate (PHRR) of the hybrids; but the introduction of TPOSS induces the ignition of the hybrids. And the addition of 2 wt% TPOSS and 3 wt% BDP leads to the maximum decrease of the PHRR. The char residues of the pure PC and the several hybrids were explored by the scan electronic microscopy (SEM) and X-ray photoelectron spectroscopy (XPS). The incorporation of both BDP and TPOSS enhances the thermal-oxidative stability and fire resistance of the char layer which builds up on the surface of the burning polymer.

**Acknowledgement** This study was financially supported by the National Natural Science Foundation of China (No. 50403014), and the National 11th five-year Program (No. 2006BAK06B06).

## References

1. Pham HT, Munjal S, Bosnyak CP (1997) In: Olabisi O (ed) Handbook of thermoplastics. Marcel Dekker, New York
2. Lee LH (1964) *J Polym Sci A* 2:2859
3. Bozi J, Czegeny Z, Meszaros E, Blazso M (2007) *J Anal Appl Pyrol* 79:337
4. Puglisi C, Sturiale L, Montaudo G (1999) *Macromolecules* 32:2194
5. Montaudo G, Carroccio S, Puglisi C (2002) *J Anal Appl Pyrol* 64:229
6. Davis A, Golden JH (1967) *Macromol Chem* 110:180
7. Jang BN, Wilkie CA (2005) *Thermochim Acta* 426:73
8. Levchik SV, Weil ED (2005) *Polym Int* 54:981
9. Liu S, Ye H, Zhou Y, He J, Jiang Z, Zhao J, Huang X (2006) *Polym Degrad Stabil* 91:1808
10. Zhou W, Yang H, Zhou J (2007) *J Anal Appl Pyrol* 78:413
11. Pawlowski KH, Scharrel B (2007) *Polym Int* 56:1404
12. Fina A, Tabuani D, Carniato F, Frache A, Boccaleri E, Camino G (2006) *Thermochim Acta* 440:36
13. Liu YR, Huang YD, Liu L (2007) *Compos Sci Technol* 67:2864
14. Liu YR, Huang YD, Liu L (2006) *Polym Degrad Stabil* 91:2731
15. Zhao YQ, Schiraldi DA (2005) *Polymer* 46:11640
16. Song L, He QL, Hu Y, Chen H, Liu L (2008) *Polym Degrad Stabil* 93:627
17. Scharrel B, Hull TR (2007) *Fire Mater* 31:327
18. Zhu SW, Shi WF (2003) *Polym Degrad Stabil* 80:217
19. Li Q, Jiang PK, Wei P (2005) *J Polym Sci Poly Phys* 43:2548
20. Hsiue GH, Liu YL, Tsiao J (2000) *J Appl Polym Sci* 78:1
21. Bourbigot S, Le Bras M, Duquesne S, Rochery M (2004) *Macromol Mater Eng* 289:499
22. Liu YL, Hsiue GH, Chiu YS, Jeng RJ, Perng LH (1996) *J Appl Polym Sci* 61:613
23. Liu YL, Hsiue GH, Lan CW, Chiu YS (1997) *Polym Degrad Stabil* 56:291
24. Bourbigot S, Le Bras M, Dabrowski F, Gilman JW, Kashiwagi T (2000) *Fire Mater* 24:201